Technical Paper

ISSN 1997-1400 Int. J. Pavement Res. and Technol. 1(3):76-84

Modeling Fatigue Cracking of Asphalt Concrete Mixtures Using Viscoelastic Continuum Damage Theory and Finite Element Analysis

Sungho Mun[1], Ghassan R. Chehab[2+], Tanmay Kumar[3], and Y. Richard Kim[4]

Abstract: The development of advanced material characterization models and their implementation in finite element analysis (FEA) using sound structural models can lead to efficient design and maintenance alternatives for asphalt pavements. Particularly, characterization of asphalt concrete in tension is a crucial element for accurate prediction of cracking distresses. A viscoelastic continuum damage model (VECD) based on: (1) the elastic-viscoelastic correspondence principle using pseudostrains; (2) the work potential theory for damage modeling; and (3) the time-temperature superposition principle with growing damage has recently been developed and continuously refined. This study incorporates the VECD in a user developed FEA module to predict responses of an asphalt pavement structure. Complex modulus testing was performed for obtaining linear viscoelastic properties of asphalt concrete mixtures, while monotonic tensile strength tests were conducted for obtaining the model's damage parameters. The model was verified by using FEA for a series of loading conditions and temperatures, which were used in laboratory testing. The predictions of deformations were very close to those measured from the laboratory tests.

***Key words**: Asphalt; Complex Modulus; Continuum Damage; Linear Viscoelasticity.*

Introduction

Fatigue cracking is one of the major distresses affecting the performance of asphalt pavements. Fatigue cracks can initiate at the bottom of the asphalt concrete layer due to tensile stresses induced by flexure and propagate to the pavement surface under repeated load applications. Recent research also suggests that fatigue cracks can also initiate at the pavement surface due to tensile and shear stresses resulted from the interaction between truck tires and the pavement surface. Accurate characterization of the tensile stress-strain behavior of the viscoelastic asphalt materials of the upper layers of flexible pavements is necessary in understanding and predicting the both bottom-up and top-down fatigue cracking [1]

Background

A fundamental approach to the prediction of fatigue damage growth in asphalt pavements is two-fold. First, a material constitutive model needs to be developed. This model should be able to incorporate the effects of various conditions encountered in actual pavements such as temperature, aging, rate of loading, loading time, and rest time. Well-established theories in the discipline of materials mechanics are available for this task. The second step is to incorporate the material constitutive model into a structural model that computes stresses and strains in pavement structures. This structural model accounts for the effects of boundary conditions (such as layer thicknesses, pavement edges, bedrock, etc.) for the pavement in question.

In recent years, there has been some success in developing a mechanistic constitutive model of asphalt concrete (AC) for pavement applications. Kim et al. [2] developed a uniaxial viscoelastic continuum damage model by, first, applying the elastic-viscoelastic correspondence principle to separate out the effects of viscoelasticity. Internal state variables were then employed based on the work potential theory to account for the damage evolution under loading and the microdamage healing during rest periods. From the verification study it was found that the constitutive model has an ability to predict the hysteretic behavior of the material under both monotonic and cyclic loading up to failure, subjected to varying loading rates, random rest durations, multiple stress/strain levels, and different modes of loading (controlled-stress versus controlled-strain). Daniel and Kim [1] discovered a unique damage characteristic curve that describes the reduction in material integrity as damage grows in the AC specimen, regardless of the applied loading conditions (cyclic versus monotonic, amplitude/rate, and frequency). The model accurately predicts performance of AC mixtures up to intermediate temperatures. For high temperatures, Chehab et al. [3] demonstrated that the time-temperature superposition is valid not only in the linear viscoelastic state, but also with growing damage. This finding allows for extending the model to characterize high temperature behavior of AC mixtures under various loading conditions.

Study Objectives

[1] Senior Researcher, Highway & Transportation Technology Institute, Korea Highway Corporation, Gyeonggi-do, 445-812, South Korea.
[2] Assistant Professor, Dept. of Civil and Environmental Engineering, The Pennsylvania State University, University Park, Pennsylvania 16802, USA.
[3] Research Engineer, ARA Consultants, Sacramento, California, USA.
[4] Professor, Dept. of Civil, Construction & Environmental Engineering, North Carolina State University, Raleigh, North Carolina 27695-7908, USA.
[+] Corresponding Author: E-mail gchehab@engr.psu.edu
Note: Submitted March 21, 2008; Revised May 20, 2008; Accepted May 21, 2008.

The objective of this study is to incorporate the viscoelastic continuum damage model (VCDM) developed and progressively improved and refined [1, 2, 3] into finite element analysis (FEA). The approach follows similar works [4, 5], in which viscoelastic constitutive relationships based on the correspondence principle and work potential theory were established in finite element (FE) routines.

Parameters and material properties for the viscoelastic model are derived from stress-strain data measured from complex modulus tests (E*) and from constant crosshead-rate tests. Tests are done in uniaxial mode under direct tension on cylindrical gyratory compacted specimens. The material model is then incorporated with a structural model of a typical pavement into a FEA routine in ABAQUS. The model in FEA is used to predict the strains of monotonic tests and compare them with the measured ones for validation. The validation process verified the code for modeling the rate-dependent behavior of AC with growing damage in tension. Once validated, the model can be used with structural models in FEA to predict cracking and other distresses in asphalt pavements.

Experimental Program

Asphalt Concrete Mixtures

The Maryland 12.5mm Superpave mixture, a standard mixture used extensively as a surface course mixture in Maryland, was selected for use in laboratory experiments, which was part of the Superpave Support and Performance Models Management project, National Cooperative Highway Research Program 9-19 (NCHRP 9-19), Tasks F and G completed in 2004.. The coarse-graded Superpave mixture utilizes 100 percent crushed limestone from Maryland and an unmodified PG 64-22 binder. No lime or recycled materials are added. The optimal asphalt content is 5.1% by mass. More details about component materials and the mix design procedures are documented in the volumetric design report (NCHRP 9-19) from which this study is part.

Specimen Preparation and Geometry

Based on an extensive specimen geometry study [6], the 75mm in diameter and 150mm in height specimen was cut and cored from 150-mm by 180-mm Superpave gyratory compacted specimens. This specimen was found to give the most uniform air void distribution and specimen strains for tests in tension, and thus was selected for use in this research. This geometry is now adopted by NCHRP for the dynamic modulus test on AC mixtures in direct tension (NCHRP 9-19). Target air void content was 4% with a tolerance of ±0.5%.

Testing Setup

Two testing systems were utilized in this research. Each consists of a servo-hydraulic closed loop testing machine, a 16-bit National Instruments data acquisition board, and a set of loose-core LVDTs (Linear Variable Differential Transducer). The first system is an MTS-810 testing system with a 100kN capacity, while the other is a UTM-25 with a 25kN capacity. Both testing machines are equipped with a temperature chamber. The two systems were calibrated against each other by conducting tests on aluminum and rubber specimens.

Determination of Linear Viscoelastic Material Properties

In order to determine time-domain linear viscoelastic response, complex modulus (E^*) test is performed. Using the experimental data from the frequency-based complex modulus test, it is necessary to pre-smooth the data to eliminate the noise and waviness of the raw data [6]. Therefore, data from E^* tests were pre-smoothed using a log-sigmoidal function before conducting the time-domain Prony-series fit.

Complex Modulus Test

The complex modulus test is performed to obtain the linear viscoelastic material properties of AC mixtures. Sinusoidal loading in tension and compression sufficient to produce total strain amplitude of about 70 micro-strains was applied at six different frequencies: 20, 10, 3, 1, 0.3, and 0.1Hz. Based on earlier work [3], the 70 micro-strain limit was found not to cause significant damage to the specimen. Tests were run in tension and compression with mean stress of zero to minimize the accumulated strain at the end of cycling. For mastercurve construction, seven replicates were tested at four temperatures: –10, 5, 25, and 40°C.

From complex modulus, E^*, dynamic modulus, $|E^*|$, and phase angle, ϕ, can be determined. Also, complex modulus can be decomposed into storage and loss modulus as follows:

$$E^* = E' + iE'' \tag{1}$$

where E' is the storage modulus, E'' is the loss modulus, and i is $\sqrt{-1}$. Dynamic modulus is the amplitude of complex modulus and is defined below:

$$|E^*| = \sqrt{(E')^2 + (E'')^2}\,. \tag{2}$$

The values of storage and loss modulus are related to dynamic modulus and phase angle as follows:

$$E' = |E^*| \cos\phi \quad \text{and} \quad E'' = |E^*| \sin\phi \tag{3}$$

The dynamic modulus at each frequency is calculated by dividing the steady state stress amplitude, σ_{amp}, by strain amplitude, ε_{amp}:

$$|E^*| = \frac{\sigma_{amp}}{\varepsilon_{amp}} \tag{4}$$

The phase angle, ϕ, is associated with the time lag, Δt, between the strain input and stress response at the corresponding frequency, f:

$$\phi = 2\pi f \Delta t \tag{5}$$

Fitting Data to log-Sigmoidal Function

The storage modulus, $E'(\omega)$, can be obtained from Eq. (3) where ω represents a reduced frequency ($w = 2\pi f$) at the temperature of interest. The log-sigmoidal function $f(\omega)$, is defined as:

$$f(\omega) = E'(\omega) = a_1 + a_2 / \{a_3 + a_4 / \exp[a_5 + a_6 \log_{10}(\omega)]\} \quad (6)$$

where a_1, a_2,..., and a_6, are the coefficients determined by a iterative Levenberg-Marquardt algorithm used in this study. The appropriate coefficients of Eq. (6) are obtained by minimizing solution between storage modulus data and log-sigmoidal function and can be expressed as:

$$\text{MINIMIZE} \quad \log_{10}[E'(\omega)] - f(\omega) \quad (7)$$

where $[E'(\omega)]$ are measured values and $f(\omega)$ are fitted.

Conversion from Frequency to Time Domain

In time domain, the relaxation modulus in the form of Prony series is expressed as follows:

$$E(t) = E_\infty + \sum_{m=1}^{M} E_m \exp(-t / \rho_m) \quad (8)$$

where E_∞, ρ_m, and E_m are infinite relaxation modulus, relaxation time, and Prony coefficients respectively. In order to determine the above material coefficients from the frequency domain modulus in Eq. (6), a Fourier-transformed constitutive equation is used as follows:

$$\breve{\sigma} = \left(E_\infty + \sum_{m=1}^{M} \frac{i\omega_n \rho_m E_m}{i\omega_n \rho_m + 1} \right) \breve{\varepsilon}, \; n = 1,..., N \quad (9)$$

where $\breve{\sigma}$ and $\breve{\varepsilon}$ are defined as stress and strain in the Fourier-transform domain, with the relaxation time expressed as:

$$\rho_m \equiv \frac{\eta_m}{E_m} \quad (10)$$

where "η_m" is the viscosity.

The complex modulus can be obtained from the constitutive equation shown in Eq. (9) according to the following equation:

$$E^* = E_\infty + \sum_{m=1}^{M} \frac{i\omega_n \rho_m E_m}{i\omega_n \rho_m + 1}, \; n = 1,..., N. \quad (11)$$

From Eq. (11), the storage modulus in frequency-domain is determined by taking the real parts of the complex modulus:

$$E'(\omega_n) = E_\infty + \sum_{m=1}^{M} \frac{\omega_n^2 \rho_m^2 E_m}{\omega_n^2 \rho_m^2 + 1}, \; n = 1,..., N. \quad (12)$$

In order to obtain the time-domain relaxation modulus, the Prony-series function in Eq. (8) is determined by using the equivalent E_∞, ρ_m, and E_m shown in Eq. (12); E_∞ can be found by the limit of $E'(\omega)|_{0<\omega<<1}$. The Prony-series coefficients, E_m, are obtained based on the selected relaxation times and reduced frequencies, ρ_m and ω_n, and the following linear algebraic equation:

$$\{F\} = [E]^{-1}\{D\} \text{ or } F_m = E^{-1}_{n,m} D_n \quad (13)$$

where the column vectors, $\{F\}$ and $\{D\}$, are E_m and $E'(\omega_n)$-E_∞ respectively; the superscript "–1" denotes an inversion; the matrix, $[E]$, is defined as:

$$E_{n,m} = \sum_{m=1}^{M} \frac{\omega_n^2 \rho_m^2}{\omega_n^2 \rho_m^2 + 1}, \; n = 1,..., N \quad (14)$$

Nonlinear Material Modeling With Growing Damage

AC is modeled as a thermorheologically simple material undergoing damage which is characterized by the work potential theory. In this section, the work potential theory for viscoelastic damage mechanics is discussed in the framework of elastic damage mechanics coupled with the viscoelastic correspondence principle. The following describes: (a) the time-temperature superposition arising from thermorheological simplicity; (b) the work potential theory for damage in elastic solids; (c) the viscoelastic correspondence principle facilitating the link between the elastic damage theory and viscoelastic damage theory; and (d) the complete viscoelastic damage theory. All these theories are discussed by using experimental results presented in Fig. 1, which contains the stress-strain relationships obtained from constant crosshead strain rate tests.

Time-temperature Superposition

The time temperature superposition states that the stress-strain behavior at a particular temperature at a given strain rate is identical to the stress-strain behavior at another temperature at a modified strain rate. This modified strain rate is obtained by simply scaling the time with a temperature function (a_T) by using the following law:

$$t = a_T \cdot t_R \quad (15)$$

In the equation, t_R is the reduced time at the reference temperature (chosen at 5°C for this study), t is the time at the given temperature, and a_T is the time-temperature shift factor. For the data given in this study, the shift factor is expressed as:

$$a_T = 10^{-0.0002(Temp)^2} - 0.1308(Temp) + 0.6582$$

where *Temp* is temperature. Note that Fig. 1 contains experimental results at two temperatures, but the rates given in the figure are the reduced rates at the reference temperature of 5°C (see Table 1 for details). The reference temperature of 5°C is chosen because the viscoplastic behavior is minimal at the strain rates used. The magnified stress-strain curves in Fig. 1 clearly indicate the rate-dependent behavior of AC – the material is generally stiffer and stronger at fast rates. For the remainder of the paper, all the experiments will be viewed in the context of the reduced strain

Table 1. Reduced Strain Rate and Material Parameters of the Damage Function.

Strain Rate	Reduced Strain Rate at Reference Temp. 5°C	Initial Pseudostiffness (I)	$C(S)$
0.00003/sec at 5°C	0.00003/sec	0.81	$0.81 \cdot \hat{C}(S)$
0.000056/sec at 5°C	0.000056/sec	0.80	$0.80 \cdot \hat{C}(S)$
0.000012/sec at 5°C	0.000012/sec	1.02	$1.02 \cdot \hat{C}(S)$
0.0135/sec at 25°C	0.000026/sec	1.10	$1.10 \cdot \hat{C}(S)$
$\hat{C}(S) = \exp(-0.00228 \cdot S^{0.506})$			

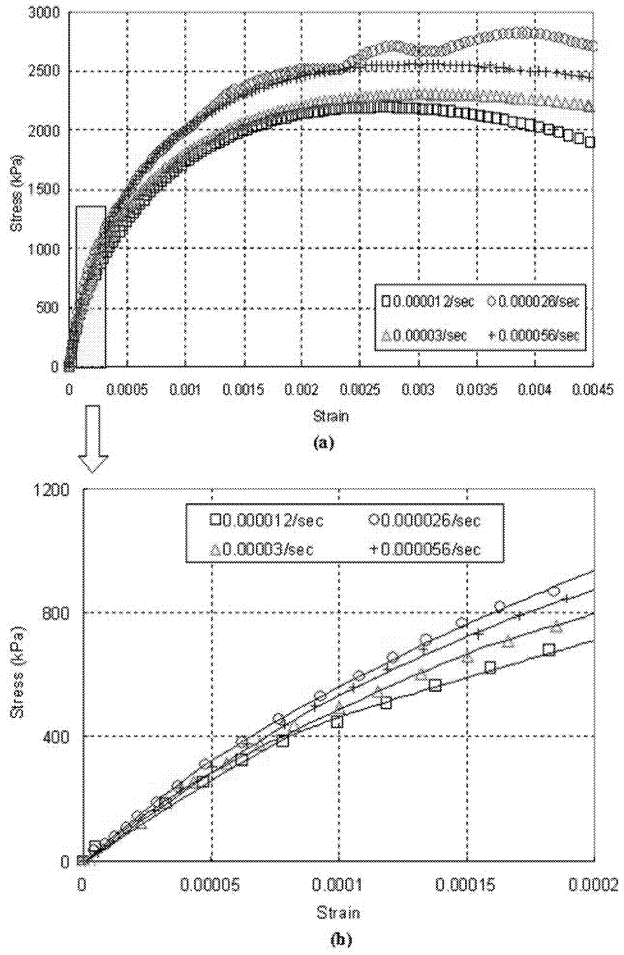

Fig. 1. Stress/Strain Curves for Varying Reduced Strain Rates in Tension Lab Tests: (a) Stress/Strain Curves up to Micro-Crack Failure; and (b) Magnified Stress/Strain Curves at Initial States.

rates at the reference temperature.

Elastic Damage Models

Schapery [7, 8] proposed a simple model for viscoelastic composites with growing damage that is based on replacing the physical displacements by quantities called pseudo-displacements. An elastic material's thermodynamic state is a function of independent generalized displacements, q_j ($j=1, 2,..., J$), and internal state variables, S_m ($m=1, 2,..., M$), where the inelastic behavior is captured from changes in S_m. Generalized forces, Q_j, are defined for each virtual displacement, ∂q , and virtual energy, ∂W , in the following form:

$$Q_j = \partial W / \partial q_j \tag{16}$$

In isothermal conditions, the virtual energy, W, is the Helmholz free energy. Therefore, W can be viewed as the strain energy depending on the strain tensor, ε_{ij}, and internal state variables, S_m. In a standard physical setting of stress and strain, Eq. (16) becomes

$$\sigma_{ij} = \frac{\partial W}{\partial \varepsilon_{ij}} \quad (i, j = 1, 2, 3) \tag{17}$$

where σ_{ij} = the stress components of the constitutive equation in the form of tensor notation.

The internal state variables are chosen to account for changes in the structure such as microcracking or macrocracking based on the following damage evolution laws:

$$-\frac{\partial W}{\partial S_m} = \frac{\partial W_S}{\partial S_m} \tag{18}$$

where $W_S = W_S(S_m)$ is the dissipated energy, a function of the damage parameter (S_m), due to damage growth. The left side of Eq. (18) is the available thermodynamic force for damage growth while the right side is the required force.

The above work potential theory is used as a guide to develop an axisymmetric constitutive relationship from the damage model. As suggested by Schapery [9], the elastic strain energy density for a local transverse isotropic composite material can be written in the following form:

$$w = \frac{1}{2}\left[A_{11}e_V^2 + A_{22}e_d^2 + 2A_{12}e_d e_V + A_{44}(\gamma_{13}^2) + A_{66}(e_S^2)\right] \tag{19}$$

where x_3 is the material axis of symmetry and $e_V = \varepsilon_{11} + \varepsilon_{22} + \varepsilon_{33}$, $e_d = \varepsilon_{33} - e_V/3$, $e_S = \varepsilon_{22} - \varepsilon_{11}$, *and* $\gamma_{13} = 2\varepsilon_{13}$ ($\gamma_{12} = \gamma_{23} = 0$ in axisymmetric model). The five coefficients (e.g., A_{11}, A_{22}, A_{12}, A_{44}, and A_{66}) are the elastic moduli depending on the state of damage. When an uniaxial stress state is taken into account with a maximum strain direction pointed to axis of x_3 (e.g., $\varepsilon_{11} = \varepsilon_{22}$, $e_S = 0$, and $\gamma_{13} = 0$), the strain energy density in Eq. (19) can be reduced to w' which is independent of A_{44}, and as shown below:

$$w' = \frac{1}{2}(A_{11}e_V^2 + A_{22}e_d^2 + 2A_{12}e_d e_V + A_{66}e_S^2) \quad (20)$$

The derivative of Eq. (20) with respect to the principal strains (e.g., ε'_{11}, ε'_{22}, and ε'_{33}) provides the principal stresses. Thus:

$$\begin{aligned}
\sigma'_{11} &= (A_{11} - \frac{1}{3}A_{12})\, e_V + (A_{12} - \frac{1}{3}A_{22})\, e_d - A_{66}\, e_S \\
\sigma'_{22} &= (A_{11} - \frac{1}{3}A_{12})\, e_V + (A_{12} - \frac{1}{3}A_{22})\, e_d + A_{66}\, e_S \\
\sigma'_{33} &= (A_{11} + \frac{2}{3}A_{12})\, e_V + (A_{12} + \frac{2}{3}A_{22})\, e_d.
\end{aligned} \quad (21)$$

The relationship between the strains, ε_{jk} ($j, k = 1, 2, 3$) in the reference coordinate system, and the principle strains, ε'_{ii} ($i = 1, 2, 3$), is given by the general second order tensor transformation below:

$$\varepsilon'_{ii} = \Omega_{ij}\Omega_{ik}\varepsilon_{jk} \quad (22)$$

where the above transformation matrix $\mathbf{\Omega}_{ij}$ is cosine(x'_i, x_j), which is the direction cosine of the axes between x'_i and x_j. A similar transformation law applies for stresses:

$$\sigma_{jk} = \Omega^T_{ik}\Omega^T_{ij}\sigma'_{ii} \quad (23)$$

where the superscript "T" denotes the transpose of a matrix and σ'_{ii} is a diagonal tensor containing the principal stresses. From earlier work [7, 8], the five coefficients, A_{11} to A_{66}, in Eq. (19) can be determined in terms of a damage function, $C(S)$, Poisson's ratio ν, and Young's modulus E:

$$\begin{aligned}
A_{11} &= \frac{1}{9}\left[C(S) + E\cdot\frac{2(1+\nu)}{(1-2\nu)}\right],\quad A_{22} = C(S) + E\cdot\frac{(1-2\nu)}{2(1+\nu)}, \\
A_{12} &= \frac{1}{3}[C(S) - E],\quad A_{44} = A_{66} = \frac{E}{2(1+\nu)}.
\end{aligned} \quad (24)$$

The damage function (C), and internal variable (S) are discussed in the following section.

Viscoelastic Correspondence Principle

Correspondence principles in linear viscoelasticity theory usually refer to elastic-viscoelastic relationships involving Laplace or Fourier transformed stresses and strains. Instead of a stress-strain constitutive equation, viscoelastic materials can be represented by an elastic-like relationship through the use of so-called pseudovariables [10]. The correspondence principles developed by Schapery for time-dependent, quasi-static solutions to nonlinear viscoelastic boundary value problems can be used to obtain a viscoelastic solution by easily constructed the elastic solution described in the above section. For linear viscoelastic materials, the stress-pseudostrain relationships take a form similar to elastic stress-strain relationships:

$$\sigma_{ij} = C^R_{ijkl}\varepsilon^R_{kl}$$

$$\text{where}\quad C^R_{ijkl} = \lambda\delta_{ij}\delta_{kl} + \mu(\delta_{ik}\delta_{jl} + \delta_{il}\delta_{jk}) \quad (25)$$

$$\text{and}\quad \varepsilon^R_{kl} = \frac{1}{E_R}\int_0^t E(t-\tau)\frac{\partial\varepsilon_{kl}}{\partial\tau}d\tau$$

C^R_{ijkl} is the material constant; $\varepsilon_{kl}{}^R$ is the pseudostrain tensor; E_R is the reference modulus; $E(t)$ is the relaxation modulus; and λ and μ are Lamé constants defined as:

$$\lambda = \frac{\nu E_R}{(1+\nu)(1-2\nu)},\quad \mu = \frac{E_R}{2(1+\nu)}. \quad (26)$$

Furthermore, ν is a constant Poisson's ratio, and δ_{ij} is the Kronecker delta:

$$\delta_{ij}\begin{cases} = 1; & i = j \\ = 0; & i \neq j \end{cases} \quad (27)$$

Note that all the hereditary effects of the viscoelastic material are accounted through the convolution integral in Eq. (25).

Viscoelastic Damage Models

Schapery further extended his elastic damage theory to viscoelastic materials with the help of the correspondence principle [10]. To include the viscoelastic effects of microcracking, he proposed the following rate-type damage evolution law:

$$\dot{S}_m = \left(-\frac{\partial W^R}{\partial S_m}\right)^{\alpha_m} \quad (28)$$

where the overdot represents the derivative with respect to time; $W^R = W^R(\varepsilon^R_{ij}, S_m)$ is the pseudostrain energy density function; α_m is a material-dependent constant; where m is not a summation. The available thermodynamic force, $-\partial W^R/\partial S_m$, is similar to a crack growth equation presented by Park and Schapery [11]. The form of the evolution law was adequate for describing the multiaxial behavior of particulate composites with growing damage [12]. In this study, this approach is applied to AC materials.

In order to determine the damage model parameter of the rate-type damage evolution, the stress responses at given strain rates and temperatures were measured, as shown in Fig. 1, under constant crosshead strain rate tests conducted on the cylindrical specimens [13]. Furthermore, LVDTs were mounted on the specimen surface to measure displacements with respect to time; the displacement was then converted into the effective strain applied to the specimen. However, the lab results obtained from experimental tests show a discrepancy between the linear strains controlled by a closed-loop servo-hydraulic MTS testing machine and the effective strains measured from the LVDT. In an attempt to ensure consistency in applying the viscoelastic theory with growing damage, the real strains obtained from the LVDTs were used for the analysis [14].

The experimental stress-strain constitutive relationship obtained from the above uniaxial tests was incorporated into the one-dimensional pseudostrain energy density function of the material in the following form:

$$W^R = \frac{1}{2}C(S)(\varepsilon^R)^2 \quad (29)$$

where the damage function, $C(S)$, depends on a single damage parameter, S. Then, the stress in Eq. (17) can be obtained based on Schapery's correspondence principle, as follows:

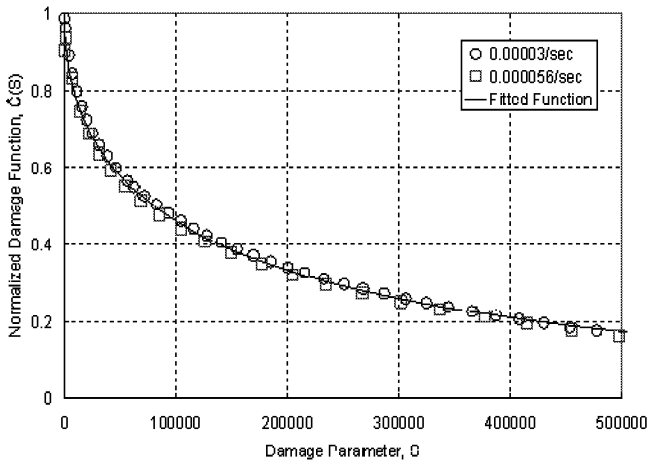

Fig. 2. Normalized Damage Function/Parameter Curves for Two Fast Reduced Strain Rates Used to Obtain a Representative Fitted Function.

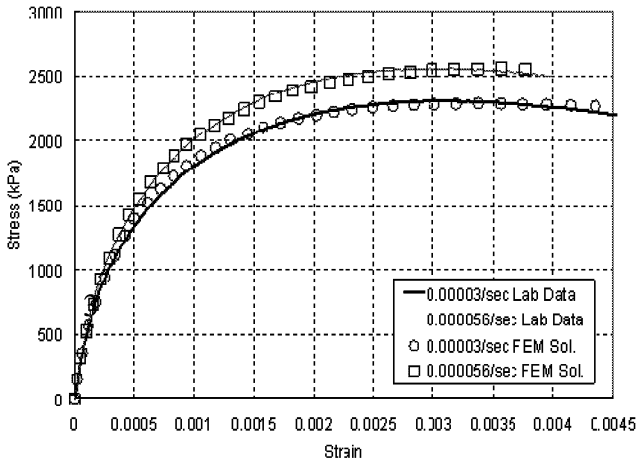

Fig. 3. Stress Prediction of 0.00003/sec and 0.000056/sec Reduced Strain Rates Used for Constructing Master Damage Function.

$$\sigma \equiv \frac{\partial W^R}{\partial \varepsilon^R} = C(S)\varepsilon^R \quad \text{or} \quad C(S) = \frac{\sigma}{\varepsilon^R} \tag{30}$$

Therefore, the damage function, $C(S)$, can be determined using the experimental stress, σ, and the pseudostrain, ε^R.

The pseudostrain is calculated by using Eq. (25). Due to the expensive nature of the convolution integral, several authors have proposed efficient integration techniques [15-18] which based on Eq. (8). Using the expression, it is shown that the convolution in Eq. (25) can be replaced by the following recursive computation [5],

$$\varepsilon_{kl}^{R,n+1} = \frac{1}{E_R}\left(E_0\varepsilon_{kl}^{n+1} - \sum_{m=1}^{M} E_m \varepsilon_{kl}^{m,n+1}\right) \tag{31}$$

with $E_0 = E_\infty + \sum_{m=1}^{M} E_m$, and

$$\varepsilon_{kl}^{m,n+1} = \varepsilon_{kl}^{n} + e^{-\Delta t_{n+1}/\rho_m}(\varepsilon_{kl}^{m,n} - \varepsilon_{kl}^{n}) + \frac{\Delta\varepsilon_{kl}^{n+1}}{\Delta t_{n+1}}\left[\Delta t_{n+1} - \rho_m\left(1 - e^{-\Delta t_{n+1}/\rho_m}\right)\right]$$

In the above, the pseudostrain is split into M pseudostrain components based on the Prony-series expansion of Eq. (8).

For uniaxial loading conditions, a single damage variable (S) is used along with the associated power, α. The value of α is obtained from the experimental data and by the following incremental relationship obtained from combining Eqs. (28) and (29):

$$\Delta S = \left[\left\{-\frac{1}{2}\Delta C(\varepsilon^R)^2\right\}^{\alpha}\Delta t\right]^{1/(1+\alpha)} \quad \text{then,}$$

$$S \equiv \sum_{n=1}^{N}\left[\frac{1}{2}(C_{n-1} - C_n)(\varepsilon_n^R)^2\right]^{\alpha/(1+\alpha)}(t_n - t_{n-1})^{1/(1+\alpha)} \tag{32}$$

Using optimization search techniques and the data from the first two cases in Table 1, the value of α is found to be equal to 2.5. Furthermore, a relationship is constructed between C and S, as shown in Fig. 2. Note that the specimen-to-specimen variation is taken into account by assuming that all the results were scaled by the initial pseudostiffness (see Fig. 3). From Figs. 2 and 3, it can be observed that the stiffness scale factor, C(S), can be fit into the normalized functional form $\hat{C}(S) = \exp(-0.00228 \cdot S^{0.506})$.

Similarly, the axisymmetric continuum damage viscoelasticity is simply obtained by using the correspondence principle in the framework of axisymmetric elastic damage mechanics. Using this idea, the pseudostrain energy density function is defined as:

$$W^R = \frac{1}{2}\left[A_{11}(e_V^R)^2 + A_{22}(e_d^5)^2 + 2A_{12}e_d^R e_V^R + A_{44}(\gamma_{13}^R)^2 + A_{66}(e_S^R)^2\right] \tag{33}$$

where

$$e_V^S = \varepsilon_{11}^R + \varepsilon_{22}^R + \varepsilon_{33}^R,\ e_d^R = \varepsilon_{33}^R - e_V^S/3,\ e_S^R = \varepsilon_{22}^R - \varepsilon_{11}^R,\ \text{and}\ \gamma_{13}^R = 2\varepsilon_{13}^R$$

($\gamma_{12}^R = \gamma_{23}^R = 0$ in axisymmetric model). In terms of principal pseudostrains,

$$W^R = \frac{1}{2}\left[A_{11}(e_V^R)^2 + A_{22}(e_d^R)^2 + 2A_{12}e_d^R e_V^R + A_{66}(e_S^R)^2\right] \tag{34}$$

Results shown below are constitutive relationships between stress and pseudostrain.

$$\begin{aligned}
\sigma'_{11} &= (A_{11} - \frac{1}{3}A_{12})e_V^R + (A_{12} - \frac{1}{3}A_{22})e_d^R - A_{66}e_S^R \\
\sigma'_{22} &= (A_{11} - \frac{1}{3}A_{12})e_V^R + (A_{12} - \frac{1}{3}A_{22})e_d^R + A_{66}e_S^R \\
\sigma'_{33} &= (A_{11} + \frac{2}{3}A_{12})e_V^R + (A_{12} + \frac{2}{3}A_{22})e_d^R.
\end{aligned} \tag{35}$$

Results and Finite Element Implementation

Due to the nonlinear nature of damage, Newton-type iterative methods are needed to solve the equilibrium equations. The tangent stiffness matrix needed in the solution procedure is often obtained by the tangent modulus relating the infinitesimal increase in the

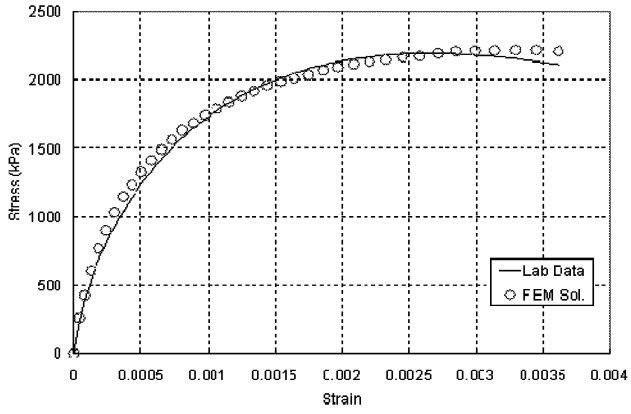

(a)

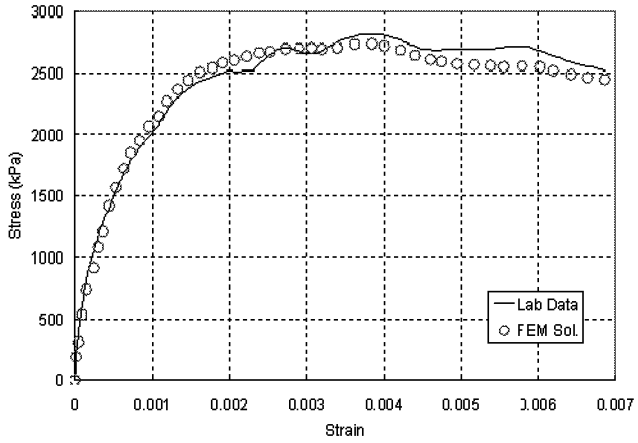

(b)

Fig. 4. Stress Prediction Compared to Measured Stress in Lab Tests: (a) 0.000012/sec Reduced Strain Rate; and (b) 0.000026/sec Reduced Strain Rate.

stress to the infinitesimal increase in the strain. For damaged viscoelastic solids, the tangent modulus is obtained using the following chain rule based on the ideas of the correspondence principle:

$$C_{ijkl} = \frac{\partial \sigma_{ij}}{\partial \varepsilon_{kl}} = \frac{\partial \sigma_{ij}}{\partial \varepsilon_{kl}^{R}} \cdot \frac{\partial \varepsilon_{kl}^{R}}{\partial \varepsilon_{kl}} \tag{36}$$

For linear viscoelasticity, the terms on the right side of the above equation are given by:

$$\frac{\partial \sigma_{ij}}{\partial \varepsilon_{kl}^{R}} = C_{ijkl}^{R}$$

and

$$\frac{\partial \varepsilon_{kl}^{R}}{\partial \varepsilon_{kl}} = \frac{1}{E_R}\left\{ E_\infty + \frac{1}{\Delta t_{n+1}}\left[\sum_{m=1}^{M} \rho_m E_m (1 - e^{-\frac{\Delta t_{n+1}}{\rho_m}}) \right] \right\} \tag{37}$$

where C^{R}_{ijkl} is defined in Eq. (25). Noting that in Eq. (25), E_∞, E_m, and ρ_m are all constants, it is observed that the tangent modulus for linear viscoelastic solids is dependent only on the time step size Δt_{n+1}.

To obtain the tangent modulus for growing damage, the chain rule (Eq. (36)) is modified in terms of the work potential as follows:

$$C_{pprr} = \frac{\partial \sigma'_{pp}}{\partial \varepsilon_{rr}^{R}} \cdot \frac{\partial \varepsilon_{rr}^{R}}{\partial \varepsilon_{rr}} = \frac{\partial^2 W^{R}}{\partial^2 \varepsilon_{rr}^{R}} \cdot \frac{\partial \varepsilon_{rr}^{R}}{\partial \varepsilon_{rr}}$$

and

$$C_{1313} = \frac{\partial^2 W^{R}}{\partial^2 \gamma_{13}^{R}} \cdot \frac{\partial \gamma_{13}^{R}}{\partial \gamma_{13}} \tag{38}$$

($C_{1212} = C_{2323} = 0$ in axisymmetric model)

The terms $\partial \varepsilon_{rr}^{R} / \partial \varepsilon_{rr}$ and $\partial \gamma_{13}^{R} / \partial \gamma_{13}$ are all related to the definition of the pseudostrain, which is identical to the pseudostrain in the linear viscoelastic case; Eq. (37) can be readily applied to compute these terms. The pseudostiffness, $\partial^2 W^{R} / \partial^2 \varepsilon_{rr}^{R}$, is obtained by using an incremental form of Eq. (33). The pseudostiffness can be expressed in terms of the coefficients of the $C(S)$ damage function A_{11}, A_{12}, A_{22}, and A_{66}, (Eq. (24)).

Once the tangent stiffness is obtained from Eq. (38) in the principal stress directions, a standard fourth order tensor transformation can be used to obtain the tangent stiffness in the original coordinate system:

$$C_{ijkl} = \Omega_{ip}\Omega_{jq}\Omega_{kr}\Omega_{ls} C_{pqrs} \tag{39}$$

where Ω_{nm} is the rotation tensor given in Eq. (22).

The procedure described above is implemented in the viscoelastic continuum damage FE program. Essentially, the FE program solves the equilibrium equations with the help of a Newton-type iterative method. Following steps are involved in the implementation:

1. Calculate the pseudostrain using the numerical integration scheme in Eq. (31); using these strains, determine the principal pseudostrains as well as the transformation matrix in Eq. (22).
2. Calculate principal stresses, which are functions of material coefficients (e.g., A_{11}, A_{22}, A_{12}, and A_{66}) and the pseudostrain; transform the principal stresses back to the stresses in the reference Cartesian coordinate (x_1, x_2, x_3) system using the transformation matrix. These stresses are used to compute the residual needed for the Newton iteration.
3. Determine the components of the incremental tangent modulus using an incremental form of Eq. (39).
4. Update the damage parameter, S, using an incremental form of the rate-type evolution law (Eq. (28)) and the definition of pseudostrain energy density (Eq. (34)). The resulting updated procedure is given below:

$$\Delta S_{n+1}^{update} = \left\{ -\frac{\left[W'^{R}(S_n + \Delta S_{n+1}^{assumed}) - W'^{R}(S_n) \right]}{\Delta S_{n+1}^{assumed}} \right\}^{\alpha} \Delta t_{n+1}$$
$$S_{n+1} = S_n + \Delta S_{n+1}^{update} \tag{40}$$

The above steps are embedded in the equilibrium solution process of the FE program that gradually increases the loading to obtain the incremental response of the system.

Verification with Experimental Data

The material modeling approach presented and the FE implementation in this section are verified with the use of the experimental results presented in Fig. 1. The cylindrical test specimen is modeled with the help of axisymmetric finite elements. To save computational time, only a quarter of the cylinder is modeled by considering the symmetry of the specimen as well as the loading. As discussed before, the experimental data corresponding to 0.00003/sec and 0.000056/sec reduced strain rates are used to characterize the viscoelastic damage parameters. The resulting damage parameters are, in turn, used in the FEA to obtain the response of the cylindrical specimen. The computed results are compared with the experimental results in Fig. 3. The close match between the computed and observed results shows the accuracy of the FE implementation.

In order to verify the effectiveness of the material modeling procedure, the FEA is conducted at different reduced strain rates, 0.000012/sec and 0.000026/sec (see Table 1). The computed results are compared with those obtained from experiment in Fig. 4, where very good matches are observed.

Therefore, it can be concluded that the viscoelastic damage model and its FE implementation are fairly accurate. However, the FE model verification by applying biaxial experimental tests with confining pressure was not carried out since experimental data was unavailable.

Conclusions and Future Work

The paper presents the methodology for incorporation of a VCDM and a structural model in FEA of asphalt pavement structures. Based on AC material modeling and FE implementation in ABAQUS, a VCDM is used for the asphalt layer while a nonlinear elastic model is used for unbound soil layers. Both the FE implementation and the applicability of the damage model for AC were tested using laboratory experimental data. Complex modulus tests and constant crosshead rate damage tests were conducted in uniaxial tensile mode to determine the model parameters for the asphalt mixture used. The model, implemented in FEA, was validated using stress-strain data from a new set of laboratory tests conducted at various loading conditions.

Future work will focus on using and expanding the findings from this study and other works done by the authors to investigate the effects of asphalt-layer thickness, layer stiffness, contact pressure distribution, and load level on the stresses and fatigue-cracking mechanism in aggregate base pavements. Other applications include thermal cracking and top-down shear-related fatigue cracking. Additionally, a viscoplastic model, recently developed by the authors, will be combined with the existing viscoelastic model to form a viscoelastoplastic model. Future studies will focus on incorporating the model in FEA to predict permanent deformations in asphalt pavements.

References

1. Daniel, J. and Kim, Y.R., (2002). Development of a Simplified Fatigue Test and Analysis Procedure Using a Viscoelastic Continuum Damage Model, *Journal of Asphalt Paving Technology*, 71, pp. 619-650.
2. Kim, Y.R., Lee, H.J., and Little, D., (1997). Fatigue Characterization of Asphalt Concrete Using Viscoelasticity and Continuum Damage Theory, *Journal of Asphalt Paving Technology*, 66, pp. 520-569.
3. Chehab, G.R., Kim, Y.R., and Schapery, R., (2002). Time-Temperature Superposition Principle for Asphalt Concrete Mixtures with Growing Damage in Tension State, *Journal of Asphalt Paving Technology*, 71, pp. 559-593.
4. Ha, K. and Schapery, R., (2002). A Three-Dimensional Viscoelastic Constitutive Model for Particulate Composites with Growing Damage and its Experimental Validation, *International Journal of Solids and Structures*, 35, pp. 3497-3517.
5. Hinterhoelzl, R., (2000). Implementation of an UMAT for Solid Propellant in the FEM Program ABAQUS according to the Constitutive Law, *Research Report*, University of Texas at Austin, Austin, TX, USA.
6. Chehab, G.R., (2002). Characterization of Asphalt Concrete in Tension Using a Viscoelastoplastic Model, *Ph. D. Dissertation*, North Carolina State University, Raleigh, N.C., USA.
7. Schapery, R., (1991). Analysis of Damage Growth in Particulate Composites Using a Work Potential, *Composite Engineering*, 60, pp. 153-173.
8. Schapery, R., (1984). Correspondence Principles and a Generalized J Integral for Large Deformation and Fracture Analysis of Viscoelastic Media, *International Journal of Fracture*, 25, pp. 195-223.
9. Schapery, R., (1990). Theory of Mechanical Behavior of Elastic Media with Growing Damage and Other Changes in Structure, *Journal of the Mechanics and Physics of Solids*, 38**,** pp. 215-253.
10. Park S., Kim Y., and Schapery, R., (1998). A Viscoelastic Continuum Damage Model and its Application to Uniaxial Behavior of Asphalt Concrete, *Mechanics of Materials*, 24, pp. 241-255.
11. Park, S. and Schapery, R., (1997). A Viscoelastic Constitutive Model for Particulate Composite with Growing Damage, *International Journal of Solids and Structures*, 34, pp. 931-947.
12. Chehab, G., Kim Y.R., and Schapery, R., (2003). Characterization of Asphalt Concrete in Uniaxial Tension Using a Viscoelastoplastic Model, *Journal of Asphalt Paving Technology*, 72, pp. 315-355.
13. Daniel, J., Chehab, G., and Kim, Y.R., (2004). Issues Affecting Measurement of Fundamental Asphalt Mixture Properties, *Journal of Materials in Civil Engineering,* ASCE, 16**(5),** pp. 469-476.
14. Kaliske, M. and Rothert, H., (1997). Formulation and Implementation of Three-Dimensional Viscoelasticity at Small and Finite Strains, *Computational Mechanics*, 19 , pp. 228-239.
15. Poon H. and Ahmad, M., (1997). A Material Point Time Integration Procedure for anisotropic, Thermorheologically Simple, Viscoelastic Solids, C*omputational Mechanics*, 21,

pp. 236-242.
16. Simo, J. and Hughes, T.J., (1998). Computational Inelasticity, New York, Springer-Verlag.
17. Taylor, R., (1970). Thermomechanical Analysis of Viscoelastic Solids, *International Journal for Numerical Methods in Engineering*, 2, pp. 45-59.
18. Zocher, M., Groves, S., and Allen, D., (1997). A Three-Dimensional Finite Element Formulation for Thermoviscoelastic Orthotropic Media, *International Journal for Numerical Methods in Engineering*, 40, pp. 2267-2288.